BioOne COMPLETE

Magnetic phases of soils developed from igneous rocks in a climate gradient transept, Brazilian northern Amazonia

Authors: Silva, Aduan L., Araújo, Roberto C., Melo, Valdinar F., Sergio, Cássio S., and Schaefer, Carlos Ernesto G.R.

Source: Canadian Journal of Soil Science, 102(4) : 879-887

Published By: Canadian Science Publishing

URL: https://doi.org/10.1139/cjss-2021-0171

BioOne Complete (complete.BioOne.org) is a full-text database of 200 subscribed and open-access titles in the biological, ecological, and environmental sciences published by nonprofit societies, associations, museums, institutions, and presses.

Your use of this PDF, the BioOne Complete website, and all posted and associated content indicates your acceptance of BioOne's Terms of Use, available at www.bioone.org/terms-of-use.

Usage of BioOne Complete content is strictly limited to personal, educational, and non - commercial use. Commercial inquiries or rights and permissions requests should be directed to the individual publisher as copyright holder.

BioOne sees sustainable scholarly publishing as an inherently collaborative enterprise connecting authors, nonprofit publishers, academic institutions, research libraries, and research funders in the common goal of maximizing access to critical research.

Downloaded From: https://bioone.org/journals/Canadian-Journal-of-Soil-Science on 29 Mar 2024
Terms of Use: https://bioone.org/terms-of-use

Canadian Journal of Soil Science

Article

Magnetic phases of soils developed from igneous rocks in a climate gradient transept, Brazilian northern Amazonia

Aduan L. Silva[a], **Roberto C. Araújo**[a], **Valdinar F. Melo**[a], **Cássio S. Sergio**[a], **and Carlos Ernesto G.R. Schaefer**[b]

[a]Federal University of Roraima, Boa Vista, Roraima 69304-250, Brazil; [b]Department of Soil, Federal University of Viçosa, Viçosa, Minas Gerais 36570-900, Brazil

Corresponding author: **Valdinar F. Melo** (email: valdinar.melo@ufrr.br)

Abstract

Knowledge on magnetic phases and properties of magnetic minerals has wide applications in soils and in agriculture, by the possibility, and perspectives in application of rock magnetic methods in soil science and agriculture; however, their role in highly weathered soils is still unclear. We characterized the mineralogy of soils from Brazilian northern Amazonia, with emphasis on magnetic soils. Samples with varying weathering degrees were collected from four different localities, and their magnetic phases (MPs) were separated and subjected to the following analysis: X-ray fluorescence (XRF), X-ray diffractometry (XRD), and measurements of field and temperature magnetization. The chemical composition by XRF analyses revealed the predominance of Fe, Si, Ti, and Mn. The XRD analysis, using the Rietveld method, revealed the presence of hematite, goethite, maghemite, and magnetite as magnetic phases: The highest concentration of MPs was detected in an Fe-rich Typic Eutrudept (54% magnetite). Magnetization measurements of the magnetic phases showed the presence of magnetite, associated with hematite and goethite, with magnetization values and transition temperature characteristics of these minerals. The magnetization varied according to soil type, indicating different weathering processes. Soil magnetism varied as a function of parent igneous rocks, in the following order: diabase > basalt > granite. The results indicate that parent material and mineral weathering influence soil magnetism in a tropical climate.

Key words: soil weathering, soil genesis, magnetism, mineralogy

Résumé

Connaître les phases magnétiques (PM) et les propriétés des minéraux magnétiques aurait de vastes applications en pédologie et en agriculture, car on pourrait appliquer les méthodes associées au magnétisme des pierres à ces deux sciences. Néanmoins, le rôle de tels minéraux dans les sols très altérés manque de clarté. Les auteurs ont caractérisé la minéralogie des sols du nord de l'Amazonie, au Brésil, en se concentrant sur les sols magnétiques. Dans cette optique, ils ont prélevé des échantillons altérés à divers degrés à quatre endroits, puis ils en ont séparé les PM qu'ils ont analysées avec les techniques suivantes : fluorescence aux rayons X (XRF), diffractométrie aux rayons X (XRD) et détermination du magnétisme en fonction du terrain et de la température. L'analyse de la composition chimique par XRF révèle la prédominance des éléments Fe, Si, Ti et Mn. L'analyse par XRD selon la méthode de Rietveld révèle que les phases magnétiques découlent de la présence d'hématite, de goethite, de maghémite et de magnétite. La concentration la plus élevée de PM a été relevée dans un eutrudept typique riche en fer (54 % de magnétite). Après quantification, la magnétisation des phases magnétiques indique la présence de magnétite associée à de l'hématite et à de la goethite, le magnétisme et les températures de transition étant caractéristiques à ces minéraux. La magnétisation varie avec la nature du sol, signe que des mécanismes d'altération différents sont en jeu. Le magnétisme du sol fluctue d'après la roche ignée mère, qui va de la diabase au basalte, puis au granit. Les résultats de ces travaux indiquent que le matériau d'origine et l'altération des minéraux influent sur le magnétisme du sol dans les climats tropicaux. [Traduit par la Rédaction]

Mots-clés : dégradation du sol, pédogenèse, magnétisme, minéralogie

Introduction

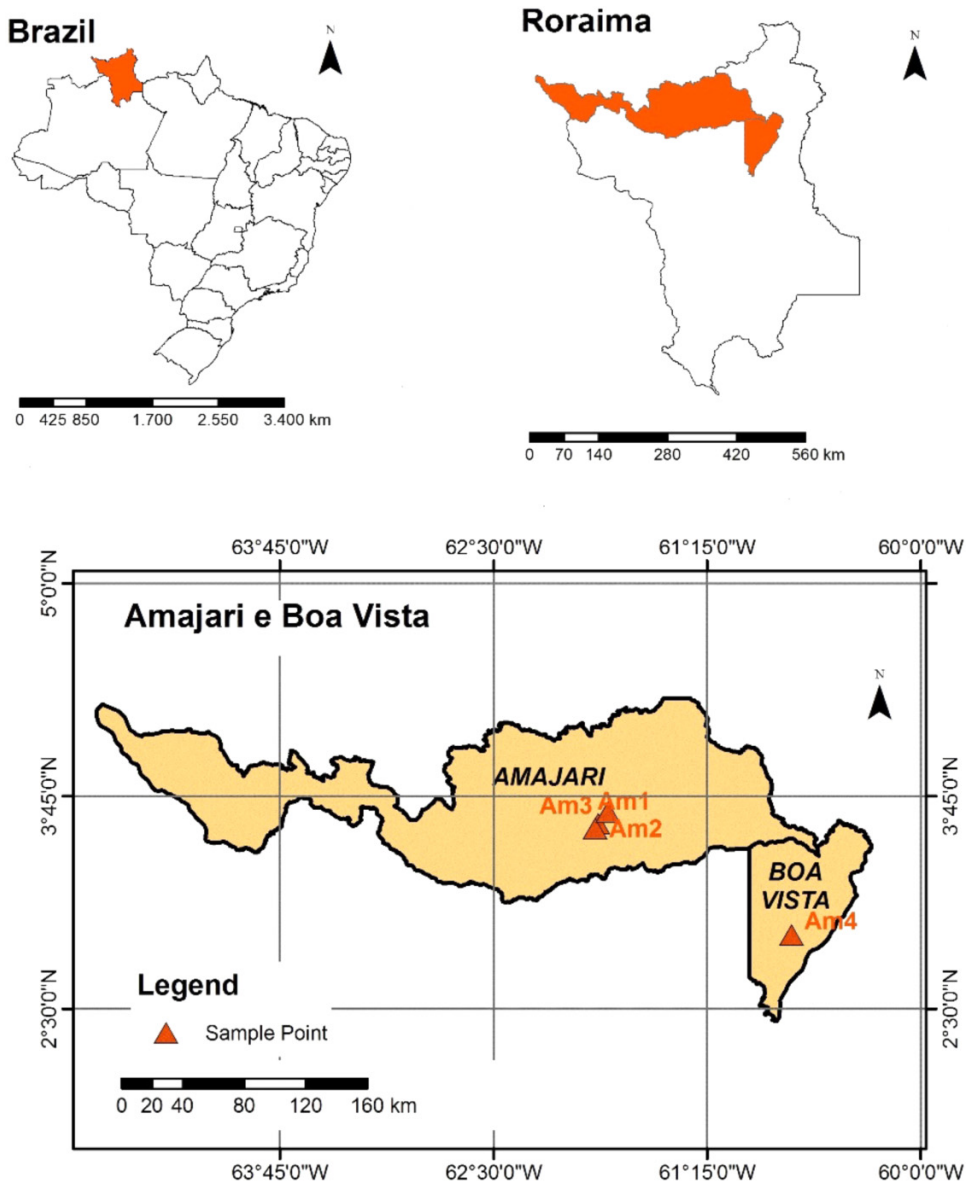
Soil magnetism is an important property, especially in tropical and subtropical soils. The development of magnetic properties results from thousands of years of natural weathering of parental rocks and minerals with crystalline iron composition (Tsambourakis et al. 1993; Dunlop and Ozdemir 1997). The basic principle of environmental magnetism involves linking magnetic properties of mineral assemblages to the environmental processes that control them, and environmental changes and climate can vary with time and in-

Downloaded From: https://bioone.org/journals/Canadian-Journal-of-Soil-Science on 29 Mar 2024
Terms of Use: https://bioone.org/terms-of-use

Table 1. Location, geographic coordinates, soil, and horizons of collected soil samples.

Soils	Parent material	Geographical coordinates	Horizons			
			A	B1	B2	B3
Hapludult	Granite	03°43′42.76″N, 61°47′43.34″W, Amajarí	0–15 cm	20–44 cm	44–75 cm	75–120 cm
Typic Hapludalf	Diabase	03°36′01.28″N, 61°53′03.43″W, Amajarí	0–10 cm	30–67 cm	67–100 cm	100–150 cm
Typic Eutrudept	Granite	03°33′43.21″N, 61°54′28.64″W, Amajarí	0–5 cm	5–28 cm	28–55 cm	55–90 cm
Ustic Endoaquert	Basalt	02°56′08.40″N, 61°45′24.03″W, Nova Olinda Hill	0–30 cm	–	–	–

Fig. 1. Localization map of the points under study in the state of Roraima (northern region of the parent materials). Map created in QGIS, version 2.18. [Colour online]



fluence the mode of sediment transport, deposition, and (or) diagenetic reaction (Liu et al. 2012). The presence and abundance of iron oxides depend on the conditions of soil evolution (Carvalho Filho et al. 2015), influencing the availability of phosphorus to plants.

In general, the minerals of major magnetic interest belong to the groups of iron oxides, iron oxyhydroxides, and some iron sulfates. However, the magnetic properties of the soil minerals depend essentially on their iron content. Because of their ferrimagnetism properties, most of the iron responsible for such behavior is found in maghemite (γ-Fe_2O_3) and magnetite (Fe_3O_4) (Costa et al. 1999). Magnetic minerals are dispersed in fine particulate soils between paramagnetic and diamagnetic minerals, clay and silicate minerals (Maher

Downloaded From: https://bioone.org/journals/Canadian-Journal-of-Soil-Science on 29 Mar 2024
Terms of Use: https://bioone.org/terms-of-use

Table 2. Semiquantitative results obtained by XRF for the studied samples.

	Elements												
	Hapludult				Typic Hapludalf				Typic Eutrudept				Ustic Endoaquert
	Ap	B1	B2	B3	Ap	B1	B2	B3	Ap	B1	B2	B3	C
Fe	35.4	34.6	29.0	33.1	37.6	37.5	36.2	54.6	60.7	60.9	53.9	67.1	50.7
Si	42.4	45.3	52.0	43.1	38.9	36.4	36.7	24.6	29.1	28.0	32.7	27.0	28.7
Al	9.8	12.4	13.2	14.1	13.8	17.8	19.8	11.0	–	–	–	–	15.8
Ti	7.5	3.1	2.6	1.2	5.6	5.7	4.8	7.4	3.0	4.0	3.6	3.2	1.9
Mn	2.2	2.4	0.9	0.5	1.3	0.6	0.5	0.6	0.7	0.5	0.3	0.4	–
K	1.5	1.4	1.5	1.2	1.2	0.8	0.9	0.5	1.1	1.0	0.6	0.4	02
S	0.3	0.4	0.3	0.3	0.2	0.2	0.2	0.2	–	–	–	–	–
Mg	–	–	–	–	–	–	–	–	0.8	0.8	0.4	0.2	0.2
V	–	0.2	0.2	0.1	0.1	0.3	0.3	0.5	0.3	0.5	0.3	0.4	–
Zr	0.0	0.1	0.2	0.2	0.1	0.1	0.1	–	0.01	0.1	0.02	–	0.3
Ca	0.2	–	0.1	–	–		–	–	4.2	4.0	3.2	0.9	1.8
Cr	0.2	0.4	0.1	0.1	0.2	0.2	0.1	0.3	–	0.3	0.4	0.2	0.1
Pb	0.1	0.1	0.1	0.1	–	–	–	–	0.2	–	–	–	–
Zn	0.1	0.03	0.0	0.02	0.1	0.1	0.1	0.03	0.1	0.1	0.1	0.1	0.1
Cu	0.1	0.05	0.1	0.02	0.1	0.1	0.1	0.04	0.1	0.1	0.1	0.1	0.1
Ag	0.1	–	–	–	–	–	–	–	–	–	–	–	–
Sr	0.03	–	0.01	–	0.01	0.2	0.1	0.3	0.1	0.1	0.0 5	0.1	0.1
Ir	0.01	0.1	0.10	–	0.01	0.1	0.01	–	–	–	–	–	–

Note: The values are given as percentages.

Table 3. Quantitative results obtained from the Rietveld method for the mineral phases detected by XRD.

	Hapludult				Typic Hapludalf				Typic Eutrudept				Ustic Endoaquert
Phase	Ap	B1	B2	B3	Ap	B1	B2	B3	Ap	B1	B2	B3	C
Qz	26.2	510	53.2	48.0	35.0	41.0	0.5	27.6	10.7	4.1	4.0	14.7	44.4
Kt	19.5	9.3	7.4	38.0	5.9	7.9	3.8	3.9	1.7	7.6	2.8	1.0	10.8
Hm	12.7	6.6	9.9	3.1	12.5	12.1	11.5	10.7	14.6	13.7	6.1	25.3	8.9
Mg	–	0.4	–	1.2	8.6	3.2	45.1	36.5	36.5	41.5	51.5	45.3	–
Mgh	–	2.2	–	–	2.1	0.7	1.2	1.7	–	–	–	–	–
Gt	16.2	14.5	12.5	3.7	0.2	4.9	6.1	3.0	–	–	–	–	11.7
Im	5.6	7.7	8.4	0.6	10.9	12.1	20.4	14.6	3.9	3.17	7.4	8.1	10.9
Bt	8.2	–	–	–	–	–	–	–	–	–	–	–	–
Msc	11.3	7.7	6.59	6.20	–	0.31	–	–	2.69	6.09	1.09	3.5	–
Ep (Zn, Fe)	–	–	–	–	24.6	19.6	–	–	–	–	–	–	–
Mgn	–	–	–	–	–	–	–	–	27.6	18.4	13.7	–	–
Mnt	–	–	–										2.1
Al	–	–	–	–	–	–	–	–	–	–	–	–	14.1
Rwg	16.1	12.6	14.1	13.8	13.7	16.9	13.0	12.8	17.2	17.5	15.7	11.7	11.8
Sig	3.1	3.6	4.1	3.9	3.20	3.23	2.7	2.8	4.3	3.9	3.4	2.6	3.0

Note: The values are given as percentages. Qz, quartz; Kt, kaolinite; Hm, hematite; Mg, magnetite; Mgh, maghemite; Gt, goethite; Im, ilmenite; Bt, bementita; Msc, muscovite; Ep, espinel (Zn, Fe); Mgn, magnesio-hornblend; Mnt, montmorilonite; Al, albite; Rwg and Sig, adjustment quality indices.

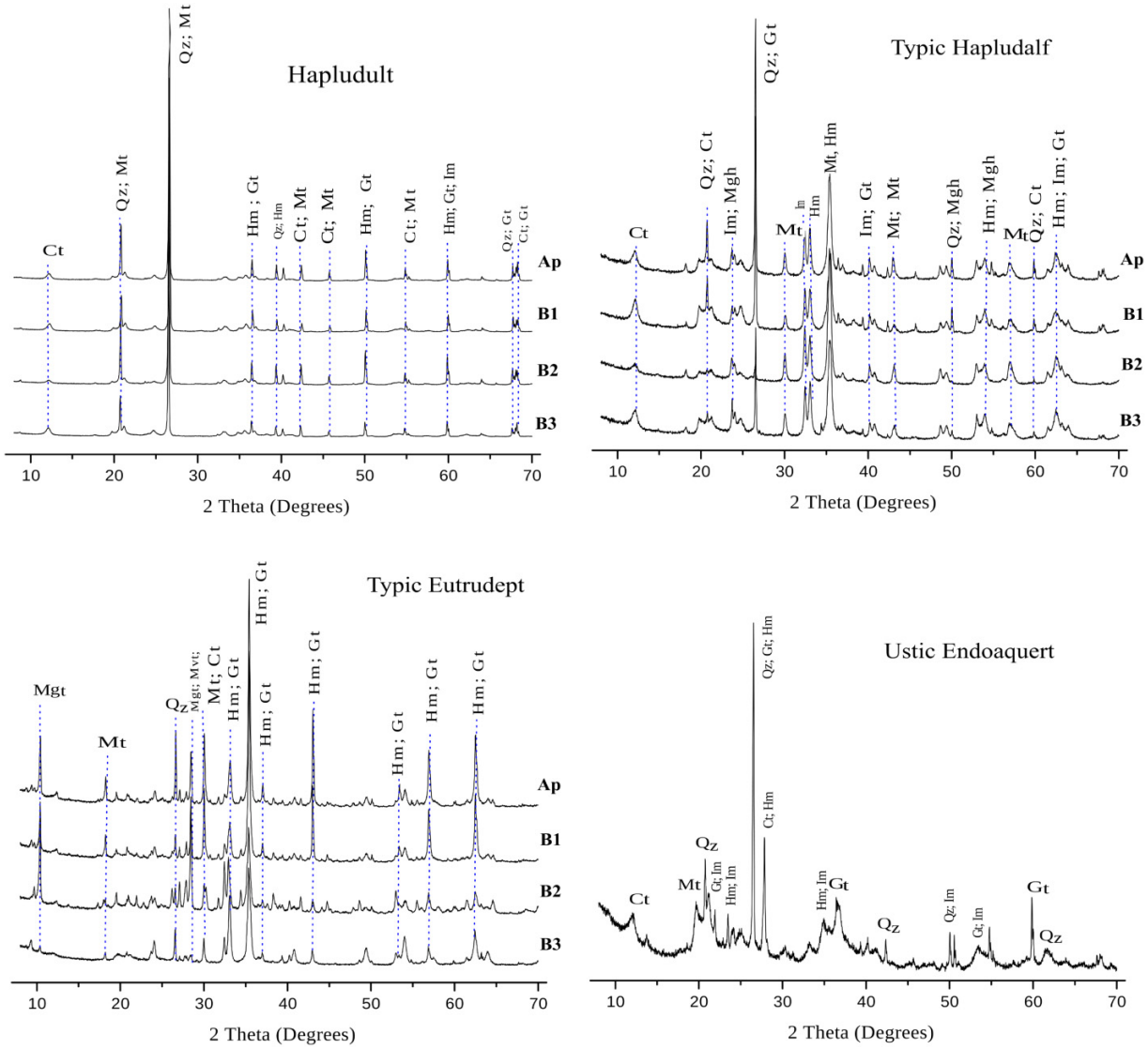
1986*b*; Cruz and Urrutia 2013). Several studies on the mineralogical characterization of magnetic minerals show that 5% of the Brazilian soils in tropical regions are magnetic (Lu et al. 2008; Jelenska et al. 2010; Cruz and Urrutia 2013; Pati and Philip 2013). Knowledge of the magnetic mineralogy of these soils is of national and global interest, as it extends from technical evaluation, via materials engineering, to the economic benefits obtained from mining industry. Currently, studies of magnetic minerals have favored both the understanding of environmental implications and the use of such minerals for the manufacture of products.

Current research on methods to distinguish magnetic minerals from natural processes, their distribution in soils, pedogenic processes involved, and elemental composition revealed a complex picture; research carried with soils from Roraima shows that soils with varying degrees of weathering are present (Melo et al. 2001). In addition, there is little knowledge of the magnetic phases in highly magnetic soils formed with weakly magnetic or nonmagnetic materials.

Soil magnetism has implications for understanding pedogenesis, the environment, pollution control, and agriculture, providing a systematic understanding of the character-

Downloaded From: https://bioone.org/journals/Canadian-Journal-of-Soil-Science on 29 Mar 2024
Terms of Use: https://bioone.org/terms-of-use

Fig. 2. X-ray diffractograms and refinement results for the selected horizons of Typic Hapludalf, Typic Eutrudept, and Hapludult. The black line represents the observed spectrum. [Colour online]



istics of Amazonian soils capable of promoting the preservation and sustainable use of natural resources. The application of the X-ray diffractometry (XRD) techniques and analysis of the behavior of magnetic compounds via magnetometry are efficient ways to characterize the mineralogy of these soils. In this context, the study of magnetization becomes relevant as it is an intrinsic property of magnetic minerals and can be studied at sufficiently high temperatures and magnetic fields, which can be indicators of physical, chemical, and mineralogical attributes of soils, beyond geochemical characterization, defining the soil genesis, and its agronomic behavior. Thus, the purpose of the present study was to determine and quantify the mineralogy and magnetic phases of different soils (Alfisol, Vertisol, Inceptsol, and Ultisol) derived from basalt, diabase, and granite in Roraima (Amazonia), by X-ray diffraction and thermomagnetic analysis.

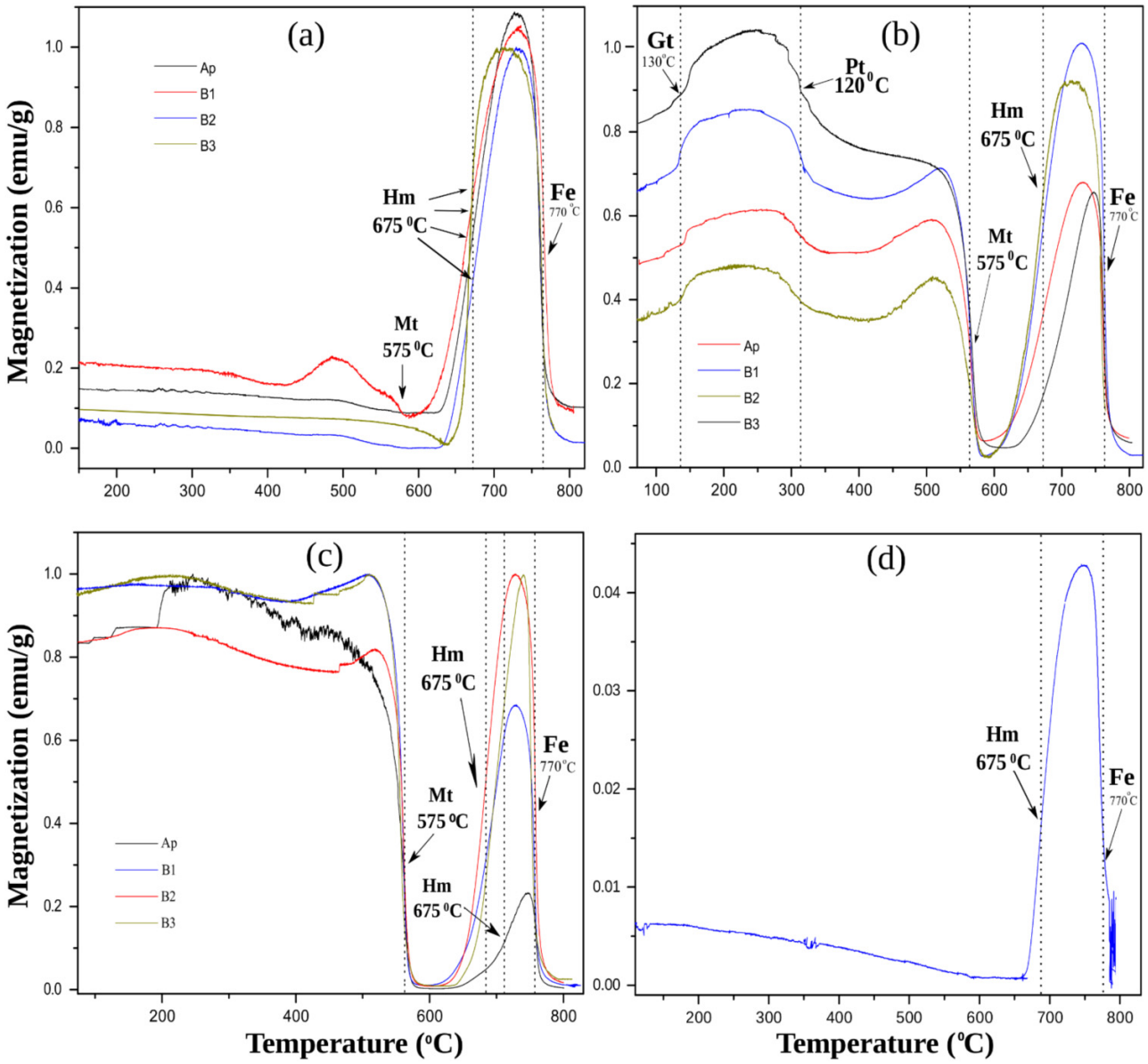
Materials and methods

Sampling and separation

Soil samples were collected in four different locations in Roraima state (Amazonia). The first three soil profiles (Site 1) were located in Amajarí, 156 km north from Boa Vista. According to the classification of Köppen, the climate of the municipality of Amajarí is classified as tropical pluvial (Af), characterized by having average temperature of the coldest month of the year greater than 18 °C, with great rainy season and short periods of drought (Peel et al. 2007), and the geology is characterized by several groups of igneous rocks interposed by mafic dikes in wave relief (Fraga et al. 2010). The fourth was located in the basaltic "Serra Nova Olinda", 10 km northeast of Boa Vista. The climate is equatorial subhumid according to the Köppen classification, with minimum temperatures of 22 °C and maximum temperatures of 39 °C.

Downloaded From: https://bioone.org/journals/Canadian-Journal-of-Soil-Science on 29 Mar 2024
Terms of Use: https://bioone.org/terms-of-use

Fig. 3. Magnetization measurements at high temperatures of selected soil horizons (A, B1, B2, and B3). Curves show strong transitions of magnetite (Mt) at 575 °C and hematite (Hm) at 680 °C. [Colour online]



Landforms are predominantly flat to slightly undulated and well drained (Barbosa 1997). The soils were classified as follows: Site 1 = Typic Hapludalf, Typic Eutrudept, and Hapludult, both under tropical rainforest; Site 2 = Ustic Endoaquert, in a flat-lying flood plain in the savanna. They were collected at four depths (0–150 cm) in their respective horizons at each site, except for the Endoaquert Ustic, which was collected from 0 to 30 cm because it was saturated by water below 30 cm, identified as surface (A) and subsurfaces (B1, B2, and B3 horizons). Table 1 shows the geographic coordinates, location, classes, and layer (surface and subsurface) horizons for all soils collected.

Soil samples were crushed and sieved using a 0.5 mm sieve. For a complete and efficient separation of the magnetic minerals from the crushed soil, the resulting fine earth was spread on a sheet of paper, using a plastic-covered supermagnet onto it. All magnetic material attached to the covered magnet was then separated and stored for subsequent analysis. This process was repeated until no material became attached to the magnet (Table 1, Fig. 1).

Chemical analyses

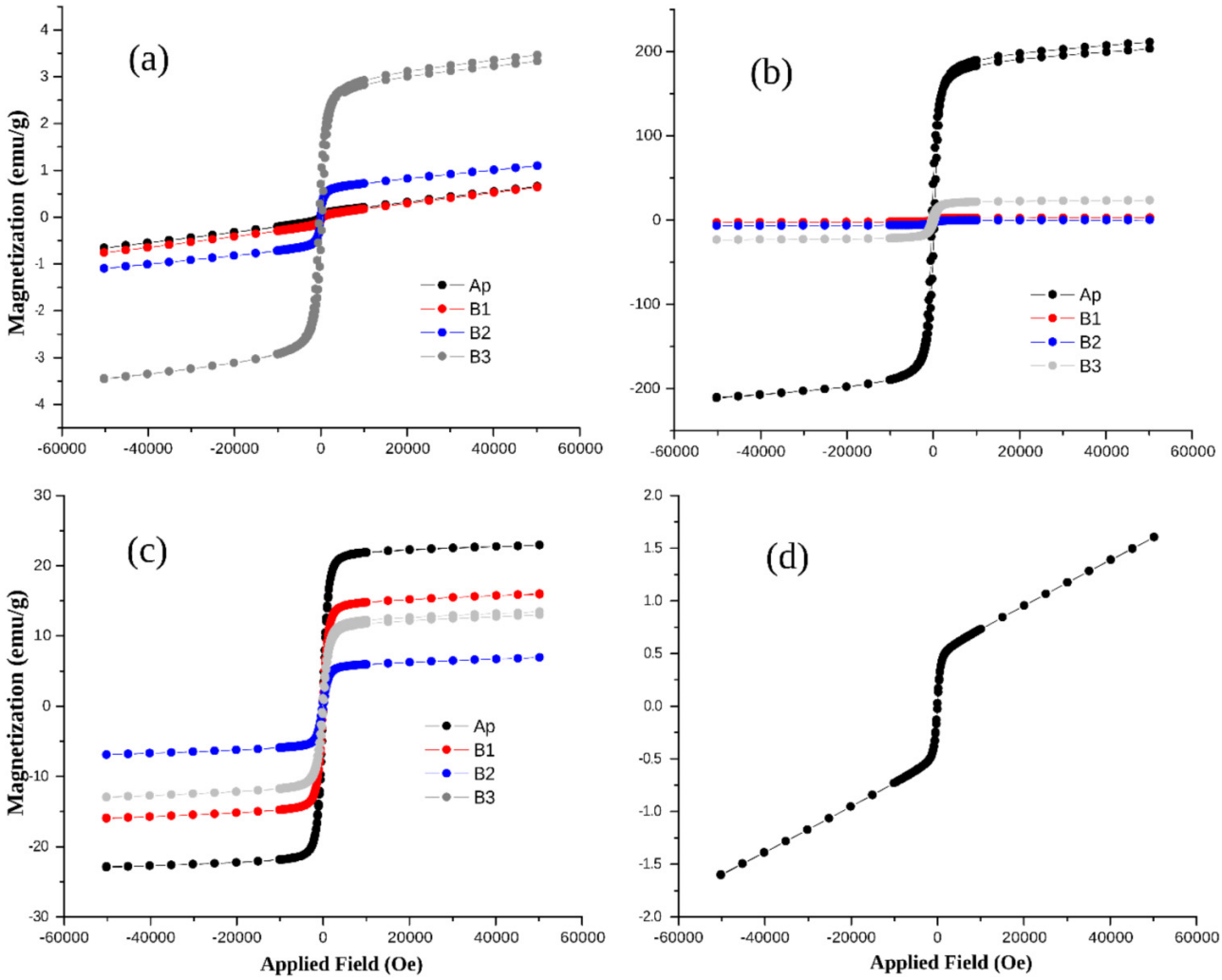
The total chemical composition (Fe, Si, Al, Ti, Mn, K, S, Mg, V, Zr, Ca, Cr, Pb, Zn, Cu, Ag, Sr, and Ir) was determined with a Shimadzu EDX-7000 X-ray fluorescence (XRF) spectrometer, equipped with a 10 mm diameter collimator. X-ray production occurred in a tube with a TG-Rh target, and a maximum voltage and current of 50 kV and 1000 mA, respectively.

Mineralogical analysis

A Shimadzu 6000 XRD Cu–Kα copper radiation emitting diffractometer was used to identify magnetic phases. During

Downloaded From: https://bioone.org/journals/Canadian-Journal-of-Soil-Science on 29 Mar 2024
Terms of Use: https://bioone.org/terms-of-use

Fig. 4. Magnetization measurements at high magnetic fields (Oe), with high coercivity indicating the presence of antiferromagnetic minerals and low coercivity indicating the presence of ferromagnetic minerals for samples of Typic Hapludalf, Typic Eutrudept, and Hapludult. [Colour online]



data collection, the equipment was operated by applying a current of 30 mA and a voltage of 40 kV to the X-ray tube; scan speed was 0.2°/minute with steps of 0.02°, with a time frame of six seconds per step. The drive shaft Bragg–Bretano geometry ($\theta/2\theta$) had a variation interval of 8–70° (2θ).

Refinement

During the calibration of the spectra obtained with the diffractometer, a free program, Material Analysis Using Diffraction (MAUD), was used for all XRD analyses, helping us to quantify and determine the crystalline structure of the samples. MAUD allows the operator to follow the refinement through Sig (S) and Rw criteria, in which an acceptable refinement must obey the following conditions: S between 1 and 2 and e Rw between 10 and 20.

Thermomagnetic analysis

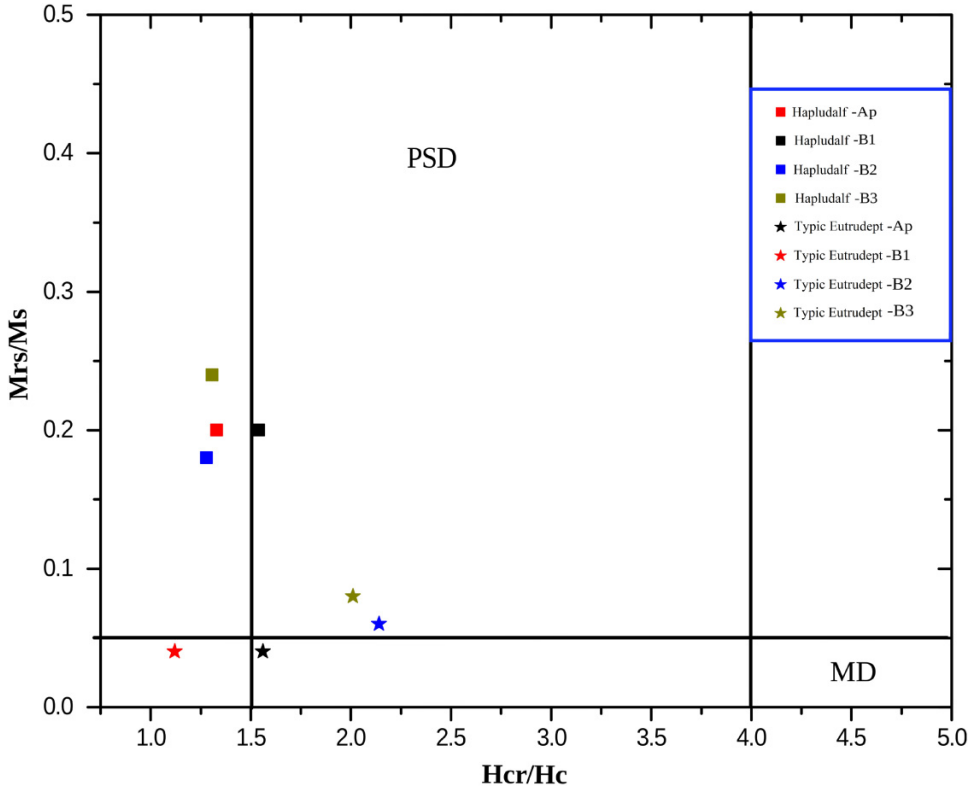
To obtain magnetization as a function of temperature, a Lakeshore vibrating sample magnetometer (VSM) was used. It has a maximum field strength of 2 T, a furnace that runs from 27 to 1000 °C, and a cryostat from −193 to 27 °C. Samples were weighed, placed in the sample port, and inserted into the VSM. Samples were run in a magnetizing field of 200 Oe, and with a temperature up to 800 °C. During heating, the magnetic ordering of each magnetic phase breaks at the Curie or Neel temperature (transition) (Pati and Philip 2013). This provides the reference point for determining the minerals responsible for the change of magnetization. However, according to the studied literature, the transitory temperature is a morphological characteristic of each material (Spinola and Spinelli 2016).

Hysteresis curves

To obtain magnetization curves as a function of the applied magnetic field (hysteresis), another magnetometer was used with a MPMS7SQUID-DC model detection system (Quantum Design). Working temperature was 2–400 K, and the maximum magnetic field was up to 7 T. For the magnetic measurements using the SQUID magnetometer, a magnetic field of up to 50 kOe was applied. Measurements were conducted

Downloaded From: https://bioone.org/journals/Canadian-Journal-of-Soil-Science on 29 Mar 2024
Terms of Use: https://bioone.org/terms-of-use

Fig. 5. Plotted Day diagram based on a schematic representation from the relation (M_{rs}/M_s versus H_{cr}/H_c) for the behavior of grain domains (PSDs, pseudo-single domain; MD, multi-domain). [Colour online]



at a 27 °C temperature, with small oscillations of 0.03 °C. From the generated curves, the following key parameters were calculated: saturation magnetization (M_s), remnant saturation magnetization (M_{rs}), coercivity (H_c), and coercivity of remanence (H_{cr}). The nature of hysteresis may indicate the presence of antiferromagnetic, paramagnetic, or diamagnetic minerals. Another important factor in hysteresis analyses concerns the state of the ferromagnetic material domains, which can be classified according to values of the ratios between magnetic parameters M_{rs}/M_s and H_{cr}/H_c. These relative proportions indicate the grain size of these particles, in the case of grains with a single domain ($M_{rs}/M_s > 0.5$; $H_{cr}/H_c < 1.5$) or grains with multidomains (MDs) ($M_{rs}/M_s < 0.1$; $H_{cr}/H_c > 3.5$). Particles within these ranges are characteristic of a simple pseudo-domain.

Results and discussion

Chemical composition

The concentrations of elements detected by XRF in the study samples (Table 2) indicate that in all soils the common major elements are Fe, Si, Al, Ti, Mn, K, and S. Si and Fe are the most abundant elements in the Hapludalf, reflecting the material (diabase). Increasing Al concentration accompanied by lower Ti concentration with depth was also recorded. In addition, the XRF detected several other metallic elements in minor concentrations, including V, Zr, Ca, Cr, Pb, Zn, Cu, Ag, Sr, and Ir. These minor elements suggest the presence of a complex chemical composition of magnetic phases. On the other hand, little variation in the concentrations of Fe, Si, Al, Ti, Mn, K, and S in soil indicates a relative homogeneity in the parental materials. The Typic Hapludalf had higher concentrations of Fe (36%–54%), Si (25%–38%), and Al (11%–208%), and lower Ti (<8%) and Mn (3%) amounts. The high iron content in the Typic Eutrudept samples may be attributed to magnetic minerals of anthropic and natural origin. The surface horizon of Ustic Endoaquert showed high levels of Fe (51%), Si (29%), and Al (16%), and similarly the presence of V, Cr, Zn, Cu, and Zr as minor metallic elements (Table 2).

Magnetic phases

X-ray diffractograms are show in Fig. 2. The overlap of peaks with high and low intensities, reflecting minor mineral components, complicates the interpretation. Samples showed distinct peaks of the magnetic phases of magnetite (Fe_3O_4), hematite (α-Fe_2O_3), maghemite (γ-Fe_2O_3), and goethite (FeO(OH)), besides nonmagnetic phases, such as quartz (SiO_2), ilmenite (FeO_3Ti), kaolinite ($Al_2Si_2O_5(OH)_4$), muscovite ($KAl_2(SiAl)O_{10}(OH,F)_2$), bementite ($H_8Mn_7O_{23}Si_6$), and spongolite ($Cu_6Al(SO_4)(OH)_{12}Cl_3(H_2O)$). Besides these, phases composed of iron as spinel ($Fe_3O_4Zn_{0.35}$), montmorillonite, nontronite, and magnesio-hornblende were also present. Magnetic properties of soils provide very sensitive proxies for the iron oxide formation, transformations, redox dynamics, and grain size of the magnetic carriers (Liu et al. 2012). In the Hapludult, only small peaks of magnetite and maghemite were detected. The presence of such phases was

Downloaded From: https://bioone.org/journals/Canadian-Journal-of-Soil-Science on 29 Mar 2024
Terms of Use: https://bioone.org/terms-of-use

expected since the XRF results had shown that samples are primarily composed of Fe, Si, Al, and Ti. The highest intensity and most prominent peak was quartz at position (26, 59, 2θ).

The Typic Hapludalf showed had very intense peaks for magnetite, maghemite, hematite, and goethite magnetic as phases. However, peaks with the highest intensity were quartz (26.5095, 2θ) and magnetite (35.4307, 2θ). The Eutrudept showed a high-intensity peak related to magnetite at around 35.4054 (2θ). In addition, the B3 horizon showed a high intensity for hematite (31.12, 2θ). In the Ustic Endoaquert, the surface horizon revealed hematite and goethite as magnetic phases (Fig. 2).

X-ray diffractograms and refinement results for the selected horizons of Typic Hapludalf, Typic Eutrudept, and Hapludult allowed the quantitative analysis of the phases in the soil samples. The black line represents the observed spectrum, the red line represents the calculated spectrum, and the green line indicates the differential spectrum.

Quantitative refinement

The Hapludult horizons and the surface of Ustic Endoaquert contained significant amounts of the magnetic phases of hematite (Table 3). In the Typic Hapludalf, the main magnetic phase was composed of magnetite (45% of B2). The Typic Eutrudept showed a high amount of magnetite, indicating a magnetic soil (Table 3). The increase in magnetic phases in soil surface can be from the parent rock during pedogenesis or from the input of atmospheric particulate fall-out of either natural or anthropogenic origin (Geiss and Zanner 2006; Fischer et al. 2008), more specifically by the process of burning vegetation.

Thermomagnetic measurements

The thermomagnetic curves for selected horizons are arranged by temperature and shown in Fig. 2. The samples showed a similar pattern, with a large magnetization increase at around 680 °C, accompanied by a decrease at around 770 °C, indicating the transition from the magnetic state of hematite to a decomposed hematite phase. Curves for Hapludult (B1), Typic Hapludalf, and Typic Eutrudept horizons show a magnetic transition at around 575 °C, related to the magnetic transition of magnetite. The Typic Hapludalf shows a transition for goethite at approximately 120 °C, and the transition for pyrrhotite magnetization loss at 320 °C (Fig. 3).

Hysteresis parameters

Magnetization curves (emu/g) based on the application of a magnetic field (Oe) to selected samples are provided in Fig. 3, which shows the main magnetic parameters of the hysteresis curves, such as the remnant magnetization of saturation (M_{rs}), coercivity (H_c), and coercivity of remanence (H_{cr}). It can be seen that samples showed differences between the hysteresis links, with well-defined ferromagnetic phases. These features are responses of the ferromagnetic material domain states, in which only iron ions contribute to magnetization (Dunlop and Ozdemir 1997). The high coercivity shown in the Hapludult and the Ustic Endoaquert (surface) indicates the contribution of the effects of antiferromagnetic minerals such as hematite and goethite, which were consistently detected in XRD. These samples did not reach a magnetization saturation, making it impossible to determine the domain regions of their magnetic carriers. Both the Typic Hapludalf and Typic Eutrudept showed low coercivity, indicating the presence of ferrimagnetic minerals of magnetite and (or) maghemite (Fig. 4).

The relationship between the magnetic parameters M_{rs}/M_s versus H_{cr}/H_c can be interpreted in the Day diagram, which indicates the grain domain regions of the analysed material (Day et al. 1997). The results indicate that the Typic Hapludalf has grains with pseudo-single domains (PSDs), whereas the Typic Eutrudept has grains with MDs at the surface and grains with PSDs in subsurface (Fig. 4). These shifts could be attributed to contribution of PSD magnetite or to a bimodal admixture of larger MD magnetite according to Dunlop (2002). It was not possible to determine the domain regions for the Hapludult or Ustic Endoaquert, since the hysteresis did not reach magnetization saturation. The Day diagram in Fig. 5 indicates the behavior of grain domains for the Typic Hapludalf and Typic Eutrudept (Fig. 5). Since H_c represents the resistance to the change in magnetization and increases generally with decreasing magnetite grain sizes, there is a smaller contribution of MD grains in the lower part of the profile (Fischer et al. 2008).

Conclusions

The results here provide insight into soils of northern Amazonia, showing variable and significant amounts of magnetic phases, and considerable concentrations of nonmagnetic phases. The Fe-rich Typic Eutrudept has highly magnetic properties related to its mafic parent material, with magnetite and maghemite as predominant ferromagnetic phases, whereas goethite is the most important antiferromagnetic phase.

The magnetization varied according to soil type and the parental igneous rock, so that the order was diabase > basalt > granite, indicating different weathering processes. Minor components without magnetic properties, such as muscovite, quartz, kaolinite, albite, sodalite, spangolite, chabazite, spinel (Zn, Fe), ankerite, and nontronite, were detected.

Acknowledgements

The authors thank Coordination for the Improvement of Higher Level Personnel (CAPES) for financial support and Dr. Adelino Aguiar Coelho from Campinas State University (Unicamp) for helping take the magnetic measurements.

Article information

History dates

Received: 17 November 2021
Accepted: 20 March 2022
Accepted manuscript online: 25 April 2022
Version of record online: 26 October 2022

Downloaded From: https://bioone.org/journals/Canadian-Journal-of-Soil-Science on 29 Mar 2024
Terms of Use: https://bioone.org/terms-of-use

Copyright
© 2022 The Author(s). Permission for reuse (free in most cases) can be obtained from copyright.com.

Data availability
Data are available on request to the corresponding author.

Author information

Author ORCIDs
Valdinar F. Melo https://orcid.org/0000-0002-7943-9969
Carlos Ernesto G.R. Schaefer https://orcid.org/0000-0001-7060-1598

Competing interests
The authors declare there are no competing interests.

References

Barbosa, R.I. 1997. Distribuição das chuvas em roraima. *In* Homem, Ambiente e Ecologia no Estado de Roraima. *Edited by* R.I. Barbosa, E. Ferreira and E. Castellón. INPA, Manaus, Brazil. pp. 325–335.

Carvalho Filho, A., Inda, A.V., Fink, J.R., and Curi, N. 2015. Iron oxides in soils of different lithological origins in ferriferous quadrilateral (Minas Gerais, Brazil). Appl. Clay Sci. **118**: 1–7. doi:10.1016/j.clay.2015.08.037.

Costa, A.C.S., Bigham, J.M., Rhoton, F.E., and Traina, S.T. 1999. Quantification and characterization of maghemite in soils derived from volcanic rocks in southern Brazil. Clays Clays Miner. **47**(4): 466–473. doi:10.1346/CCMN.1999.0470408.

Cruz, L.P., and Urrutia, J. 2013. A facile approach to enhance the high temperature stability of magnetite nanoparticles with improved magnetic property. J. Appl. Phys. **113**: 044314.

Day, R., Fuller, M., and Schmidt, V.A. 1977. Hysteresis properties of titanomagnetites: grain-size and compositional dependence. Phys. Earth Planet. Inter. **13**: 260–267. doi:10.1016/0031-9201(77)90108-X.

Dunlop, D.J., 2002. Theory and application of the Day plot (M_r/M_s versus H_{cr}/H_c). 2. Application to data for rocks, sediments, and soils. J. Geophys. Res. **107**(B3): 5–15. doi:10.1029/2001JB000487.

Dunlop, D.J., and Ozdemir, O. 1997. Rock magnetism, fundamentals and frontiers. Cambridge University Press, Cambridge, UK.

Fischer, H., Luster, J., and Gehring, A.U. 2008. Magnetite weathering in a Vertisol with seasonal redox-dynamics. Geoderma, **143**: 41–48. doi:10.1016/j.geoderma.2007.10.004.

Fraga, L.M.B., Dreher, A.M., Grazziotin, H., Reis, N.J., Farias, M.G.F., and Ragatky, D. 2010. Geologia e Recursos Minerais da Folha Vila De Tepequém – NA.20-X-A-lll Estado de Roraima, Escala 1:100.000. Serviço Geológico do Brasil – CPRM. 183p.

Geiss, C.E., and Zanner, C.W., 2006. How abundant is pedogenic magnetite? Abundance and grain size estimates for loessic soil based on rock magnetic analyses. J. Geophys. Res. **111**: B12S21. doi:10.1029/2006JB004564.

Jelenska, M.A., Hasso-Agopsowicz, A., and Kopcewicz, B. 2010. Thermally induced transformation of magnetic minerals in soil based on rock magnetic study and Moessbauer analysis. Phys. Earth Planet. Inter. **179**: 164–177. doi:10.1016/j.pepi.2009.11.004.

Liu, Q., Roberts, A., Larrasoaña, J., Banerjee, S., Guyodo, Y., Tauxe, L., and Oldfield, F. 2012. Environmental magnetism: principles and applications. Rev. Geophys. **50**: 1–50. doi:10.1029/2012RG000393.

Lu, L.S.G., Qing-Feng, X., and Jin-Yan, Z.L.Y. 2008. Mineral magnetic properties of a weathering sequence of soils derived from basalt in eastern China. Catena, **73**: 23–33. doi:10.1016/j.catena.2007.08.004.

Maher, B. 1986b. Magnetite biomineralization in termites. Proc. R. Soc. Lond. Ser. B, **42**: 76–92.

Melo, V.F., Fontes, M.P.F., Novais, R.F., Singh, B., and Schaefer, C.E.G.R. 2001. Características dos óxidos de ferro e de alumínio de diferentes classes de solos. Rev. Bras. Cienc. Solo, **25**: 19–32. doi:10.1590/S0100-06832001000100003.

Pati, S.S., and Philip, J. 2013. A facile approach to enhance the high temperature stability of magnetite nanoparticles with improved magnetic property. J. Appl. Phys. **113**(4): 314–319. doi:10.1063/1.4789610.

Peel, M.C., Finlayson, B.L., and McMahon, T.A. 2007. Updated world map of the Köppen–Geiger climate classification. Hydrol Earth Syst. Sci. Discuss. **4**: 439–473.

Spinola, T.S., and Spinelli, J.E. 2016. Transient directional solidification of cast iron: microstructure formation, columnar to equiaxed transition and hardness. Mater. Res. **19**: 795–801. doi:10.1590/1980-5373-MR-2015-0777.

Tsambourakis, F., Hill, R.J., and Madesen, I.C. 1993. Improved petrological modal analysis from X-ray powder diffraction data by use of the Rietveld method. I. Selected igneous, volcanic, and metamorphic rocks. J. Petrol. **35**: 837–900.

Downloaded From: https://bioone.org/journals/Canadian-Journal-of-Soil-Science on 29 Mar 2024
Terms of Use: https://bioone.org/terms-of-use